Climb, Cruise and Descent Speed Reduction for Airborne Delay without Extra Fuel

Yan Xu[1] Ramon Dalmau[2] and Xavier Prats[3]
Technical University of Catalonia, Castelldefels 08860, Barcelona, Spain

I. Introduction

In the majority of the situations, Air Traffic Flow Management (ATFM) regulations are issued due to weather related capacity reductions. Considering the uncertainties in weather prediction and other unforeseen factors, ATFM decisions are typically conservative and the planned regulations may last longer than actually needed [1, 2]. At present, ground delay is more preferable than airborne delay (holding) from a safety, environmental and operating cost points of view. However, when regulations are canceled before their initial planned ending time, as occur often [3, 4], the already accomplished delay on ground cannot be recovered, or can be partially recovered by increasing speed, leading to extra fuel consumption.

In order to overcome this issue, a speed reduction (SR) strategy was proposed in [5], which aimed at partially absorbing ATFM delays airborne. Ground delayed aircraft were enabled to fly at the minimum fuel consumption speed (typically slower than nominal cruise speed initially chosen by the airline) performing in this way some airborne delay. At the same time, part of the fuel was saved with respect to the nominal flight. This strategy was further explored in [6], where aircraft were allowed to cruise at the lowest possible speed in such a way the specific range (i.e., the distance flown per unit of fuel consumption) remained the same as initially planned. In this situation, if regulations were canceled, aircraft already airborne and flying slower, could increase their cruise

[1] Ph.D. candidate, Department of Physics - Aeronautics Division, Office C3-121, Esteve Terradas 5, Castelldefels, Catalonia, Spain, Email address: yan.xu@upc.edu, AIAA Student Member.
[2] Ph.D. candidate, Department of Physics - Aeronautics Division, Office C3-121, Esteve Terradas 5, Castelldefels, Catalonia, Spain, Email address: ramon.dalmau@upc.edu.
[3] Associate Professor, Department of Physics - Aeronautics Division, Office C3-104, Esteve Terradas 5, Castelldefels, Catalonia, Spain, Email address: xavier.prats@upc.edu, AIAA Member.

speed to the initially planned speed and recover part of the delay without extra fuel consumption [2, 6–8].

In this paper, the SR strategy presented in [6] is extended in such a way that not only the cruise phase is used to perform linear holding, but also the climb and descent phases are subject of optimization to maximize the total amount of airborne delay that can be achieved without incurring extra fuel cost. Three cases are studied: SR only in cruise; SR in the whole flight, but keeping the nominal cruise altitude; and SR for the whole flight while also optimizing the cruise altitude to maximize delay.

II. Methodology

A. Equivalent speeds in climb, cruise and descent

Current on-board flight management systems enable airlines to optimize the aircraft trajectory in terms of direct operating costs by means of the cost index (CI), which represents the ratio between time-based cost and the cost of fuel [9]. The higher CI is, the more importance will be given to the trip time and the faster the optimal aircraft speed will be.

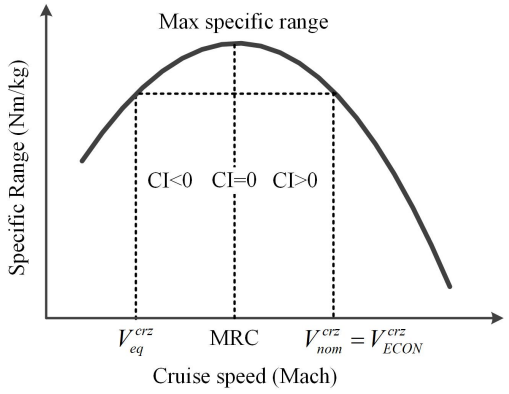

Fig. 1 Specific range as a function of cruise speed [6].

Typical operating cruise speeds are higher than the MRC (maximum range cruise) speed (i.e. the speed corresponding to CI=0), since aircraft operators also consider time-related costs when planning their flights. Accordingly, the specific range for cruise is lower than the maximum specific range for that altitude. In [6] the authors defined the equivalent speed V_{eq}^{crz} for cruising as the minimum speed that produces the same specific range as flying at the nominal speed $V_{nom}^{crz} = V_{ECON}^{crz}$.

Therefore, for all speeds between V_{eq}^{crz} and V_{nom}^{crz}, as shown in Fig. 1, the fuel consumption will be the same or lower than initially planned while the flight time in cruise will be higher.

Not only is the cruise phase affected by CI, but also climb and descent phases. With CI increasing, the speed of both climb and descent increases, as well as fuel consumption, and the climb profile becomes shallower, while conversely the descent profile turns steeper (see Fig. 2) [10].

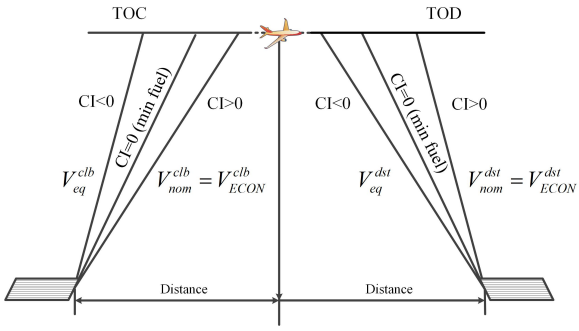

Fig. 2 Climb and descent profiles versus cost index.

Thus, the SR strategy could be extended to the whole flight and not just the cruise phase, in order to increase the amount of airborne delay and even make it appealing for short-haul flights, as climb and descent often represent a considerable percentage of the total trip distance. A similar behavior than in cruise occurs for climb and descent phases when a CI higher than 0 is selected by the operator. In such case, the climb and descent speeds are faster than those of minimum fuel for each phase as a whole, and there exists an equivalent speed $V_{eq}^{clb/dst}$ yielding the same fuel consumption as $V_{nom}^{clb/dst}$.

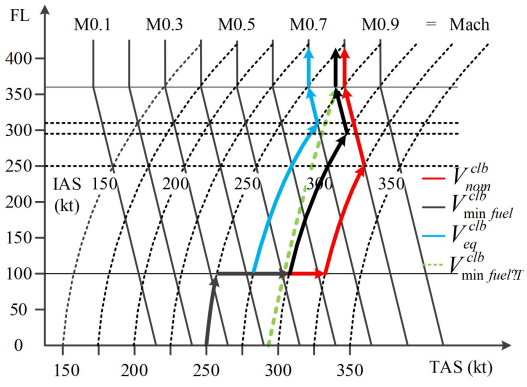

Fig. 3 Speed profiles under conventional operation constraints.

For a given aircraft, the theoretical minimal fuel speed $V^{clb}_{minfuelT}$ is not constant and changes with altitude (and with aircraft mass as long as fuel is burned). This speed is denoted with a green dashed line in Fig. 3, for a hypothetical climb.

In real operations this speed is not followed, due to operational or ATM constraints. Unlike in cruise where flight is performed at a constant Mach number, the climb is divided into several speed segments. These typically include a speed limitation at low altitudes, typically 250kt IAS (indicated airspeed) below FL100, followed by an acceleration to a constant IAS climb, followed by a constant Mach climb above the crossover altitude. Fig. 3 shows an example for such a climb speed profile (250kt/300kt/M0.78 for this example) with a solid black line and denoted in this paper as $V^{clb}_{minfuel}$.

Nominal climb speeds for CI greater than zero will lead to climb speed profiles as shown by the red line in Fig. 3 (V^{clb}_{nom}), while V^{clb}_{eq} denotes the equivalent climb speed profile leading to the same fuel consumption. As for descent, the realistic speed profile is just like the one of climb, but in opposite order that is from constant Mach descent above crossover altitude to the deceleration process at low altitudes.

As the cruise speed reduces, in general, the optimal flight level decreases. Since the equivalent cruise speed V^{crz}_{eq} is lower than the nominal cruise speed V^{crz}_{nom}, it is possible that the initial planned flight level is no longer the optimal in SR cases. When a new flight level exists, by which the specific range keeps the same or higher while speed reduces more, then it could replace the nominal one. Furthermore, if the new flight level decreases, more fuel can be saved for climb and descent due to the altitude reduction of the TOC and TOD. Thus, the objective of allowing altitude changes is to achieve more airborne delay by the same amount of fuel consumption, namely finding the altitude and speed combination (through trajectory optimization as presented in Sec. II B) that results in that same specific range with the lowest possible speed.

Moreover, worth noting that the equivalent speeds in climb, cruise and descent might be limited by the minimum operational speed (including possible safety margins). In this paper, the Green Dot (GD) speed is adopted as the minimum bound, which depicts the best lift to drag ratio speed in clean configuration. In manual flight, the selected speed/Mach could be set to VLS (lowest selectable speed, the stalling speed at 1.3g) that is lower than the GD speed. Yet, considering the operation

of the SR strategy and aiming at automatic flight, it is more realistic to choose the managed mode and therefore GD as the lower bound for speed. According to [11] GD speed, below FL200 equals to 2 $\times$ *weight* (tons) + 85 (kt), and above FL200, adds 1 kt per 1000ft.

B. Trajectory optimization of the four cases of study

As discussed above, the equivalent speeds depend not only on nominal speeds, but also the functions of fuel consumption, which in turn are aircraft performance (such as different types of aircraft models), atmospheric magnitudes (i.e., temperature, pressure and wind parameters) and flight status (e.g., aircraft mass which reduces progressively) dependent, and should change continuously along the execution of a particular flight.

In [6], an approximation was made with regards to these changes by using average values from the initial and final flight status, such as the mass of aircraft. This could apply for normal cruise phase which maintains relatively constant changes, but when taking climb and descent phases involved, it is more accurate to implement the continuous optimization to formulate this optimal control problem of performing SR within the whole flight phases, as has been studied in [12].

In this paper, optimal trajectories computed with a given CI would be regarded as the *nominal flights*, and labeled as Case-0. Based on Case-0, different SR strategies will be analyzed, denoted by Case-1, Case-2 and Case-3:

Case-1: SR in cruise maintaining the nominal flight level;

Case-2: SR in climb, cruise and descent maintaining the nominal flight level; and

Case-3: SR in climb, cruise and descent and optimizing for cruise flight level.

The optimization of aircraft trajectory requires the definition of a model capturing aircraft dynamics and performances, along with a model for certain atmospheric criteria. In this paper, a point-mass dynamics model, an enhanced performance model using manufacturer performance data and the International Standard Atmosphere (ISA) have been considered. For more details, the readers may refer to [13].

The objective of the optimization for Case-0 is to minimize the cost function consisting of fuel F and time T, with different CI values, as Eq. 1, while satisfying the optimization constraints that

model current operational procedures.

$$\min(\sum F + CI \cdot T) \tag{1}$$

The conventional flight profile is divided into several segments where different models and standard operational procedures apply. Fig. 4 summarizes the segments and the corresponding path and event constraints.

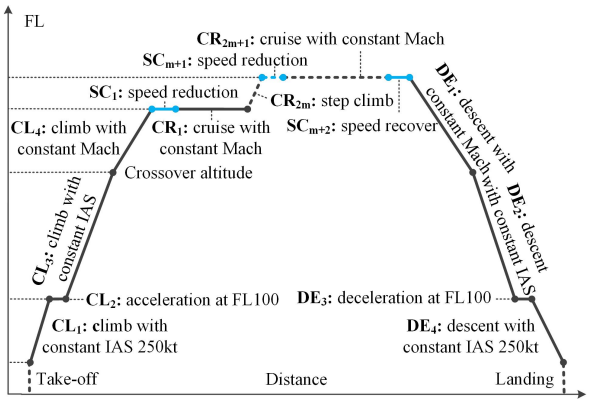

Fig. 4 Operational flight profiles divided into specific segments.

For the SR Cases, consider that the basic optimization objective and constraint are as follows:

$$\max(\sum T_i^{clb} + \sum T_j^{crz} + \sum T_k^{dst}) \tag{2}$$

$$\sum F_i^{clb} + \sum F_j^{crz} + \sum F_k^{dst} \leq F_{nom} \tag{3}$$

where i, j, k represent the segments that each phase is divided, as denoted in Fig. 4. T^{clb}, T^{crz}, T^{dst} are the time needed for climb, cruise and descent respectively, and F^{clb}, F^{crz}, F^{dst} denote the fuel consumed for each phase while F_{nom} is the fuel as initial planned in the nominal flight. Note that for Case-1 T^{clb} and T^{dst} are not subject to optimization and are fixed to the nominal climb and descent times, respectively.

Since typically the cruise speed is constant Mach, in order to realize the SR in practice, an extra segment is added in front of each cruise phase allowing speed changes (see SC_1, SC_{m+1} in Fig. 4),

as well as a similar segment (SC_{m+2}) at the end of the last cruise phase.

In addition to the flight profile, a flight route must be defined either in Great Circle Distance (GCD) between city-pair airports, or by using ATM service route and published procedures.

To find the optimal solution of the formulated optimal control problem, direct collocation methods [14] are used in this paper, which discretize the time histories of control and state variable at a set of nodal or collocation points, transforming the original continuous (infinite) optimal control problem into a (discrete and finite) nonlinear programming (NLP) optimization problem. The new finite variable NLP problem is solved by using solvers CONOPT (as NLP) and SBB as MINLP (mixed integer nonlinear programming), both bundled into the GAMS software suite. The whole process is briefly presented in Fig. 5.

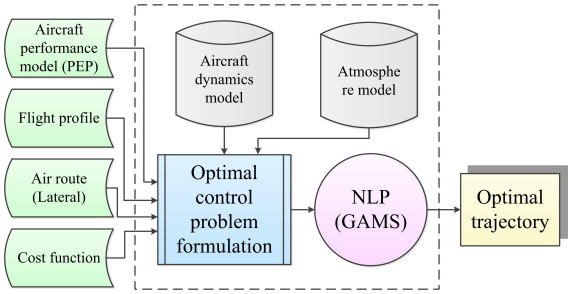

Fig. 5 Main process in generating the optimal aircraft trajectory.

III. Illustrative Examples

Results have been obtained from an in-house trajectory optimization tool, firstly with a particular flight AMS-SVQ with CI=150 analyzed in detail, along with its vertical trajectories and speed profiles illustrated specifically. Then, more representative routes are included into comparison and each is further studied with different CI values. Airbus A320, a common two-engine narrow-body transport aircraft is the aircraft type for this simulation. Airbus A320, a common two-engine narrow-body transport aircraft, has been used for this computational experiment.

Some assumptions have been taken: 1) GCD is considered; 2) a passenger occupation (payload factor) of 81% is considered for all flights [6]; 3) no wind conditions are considered; 4) alternate and reserve fuel are not included; 5) even flight levels are used (FL260 as the lowest altitude); and 6) cruise step climbs are allowed with 2000ft steps for each flight level.

A. Trajectories of a specific flight: AMS-SVQ with CI=150

The vertical trajectories corresponding to the four Cases of the AMS-SVQ: CI=150 flight are as shown in Fig. 6. The changes when SR is implemented in climb and descent phases can be appreciated in the profile, while the optimal flight level for Case-3 decreases from FL340 to FL320. Comparing the blue dots (Case-2) with the red ones (Case-0), we find the aircraft is climbing steeper (recall that the cruise flight level keeps unchanged for this Case), saving some fuel in the climb phase while also delaying the flight. Conversely, the descent is performed more gradually and flying slower, but burning some extra fuel if compared with Case-0. As for the green squares (Case-3), a decrease in cruise flight level generates even steeper climb and shallower descent trajectories. Table 1 illustrates clearly these changes for all Cases of study.

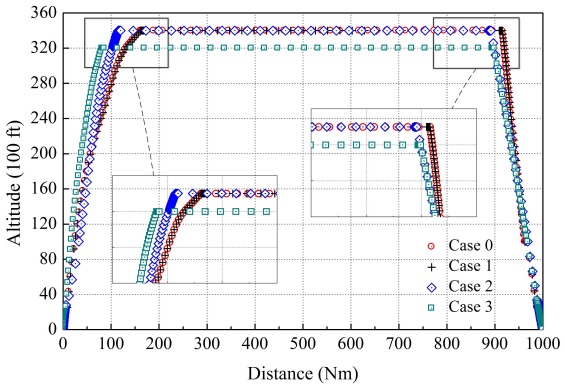

Fig. 6 Optimal trajectories generated for each Case.

Table 1 Details of a specific flight for climb, cruise and descent.

Cases	Climb phase				Descent phase			
	Fuel (kg)	Time (min)	Dist (nm)	Avg V (kt)	Fuel (kg)	Time (min)	Dist (nm)	Avg V (kt)
Case 0	1685.4	21.5	157.3	438.0	107.2	12.6	75.6	359.7
Case 1	1685.4	21.5	157.3	438.0	107.2	12.6	75.6	359.7
Case 2	1415.8	23.3	110.7	285.1	183.5	22.8	99.5	261.4
Case 3	1064.4	13.7	76.4	335.3	176.0	21.5	92.8	258.5

Cases	Cruise phase						Total	
	FL (100ft)	Fuel (kg)	Time (min)	Dist (nm)	SR (nm/kg)	Avg V (kt)	Fuel (kg)	Time (min)
Case 0	340	4006.5	97.8	754.3	0.1883	462.6	5799.1	132.0
Case 1	340	4006.5	120.2	754.3	0.1883	376.6	5799.1	154.3
Case 2	340	4199.8	156.8	777.1	0.1850	297.4	5799.1	202.9
Case 3	320	4558.8	168.5	818.1	0.1795	291.3	5799.1	203.7

Compared with the nominal flight (Case-0), Case-1 consumes the same amount of fuel in each phase and achieves 22 minutes of airborne delay when cruising, which accounts for the 22% of the

cruise time and the 17% of the total time.

In Case-2, the fuel consumption reduces 270kg (16%) in climb and the airborne delay is almost 2 minutes in this phase. Since the total fuel consumption is the same for the flight, the 270kg of fuel saved in climb can actually be allocated in cruise (193kg, 5% of cruise) and descent (77kg, 71% of descent), which, in fact, allows to largely increase the time delayed in both phases: 59 minutes (60% of cruise) and 10 minutes (77% of descent), respectively. As a result, if we compare Case-2 with Case-1, it seems that a 193kg (5%) increase of fuel consumption in cruise could exchange for 37 minutes (31%) more time delayed.

Regarding Case-3, when cruise flight level is allowed to change, the new optimal altitude (FL320) allows the aircraft to perform more airborne delay with the same fuel consumption than in Case-0 (nominal Case). Compared to Case-2, 351kg (25%) of fuel are saved during the climb phase, 8kg (4%) of fuel during the descent phase, and 359kg (9%) of fuel are added to the cruise phase, lowering the specific range by 0.006 nm/kg, and further reducing the equivalent cruise speed to produce an even longer (12 minutes) air delay in cruise. Although the flight time in both climb and descent are shorter, the total flight time increases (by 1 minute) due to this extended cruise flight time.

B. Climb, cruise and descent speed profiles

As we can tell from Fig. 7(a), the climb speed profiles of all the Cases have quite similar structures, which mainly include a continuous acceleration process at low altitude, a constant IAS climb, followed by constant Mach climb at higher altitudes. At the end of the climb a small deceleration is observed in order to reach the (reduced) optimal cruise speed. Making Case-0 as the baseline, the difference with Case-1 only lies on the deceleration process at cruise flight level, so they share exactly the same climb speed (see Table 1).

In Case-2 when SR is allowed in climb (and descent), the optimizer chooses a climb speed around 210kt (instead of the 330kt observed in Case-0), as is the minimum speed allowed (GD speed). Due to this lower IAS climb, a higher crossover altitude (around FL320) is obtained to switch to the climb Mach number, which is also lower than the nominal one.

Results show that the climb speed in Case-3 is higher than the GD speed used in Case-2 (see

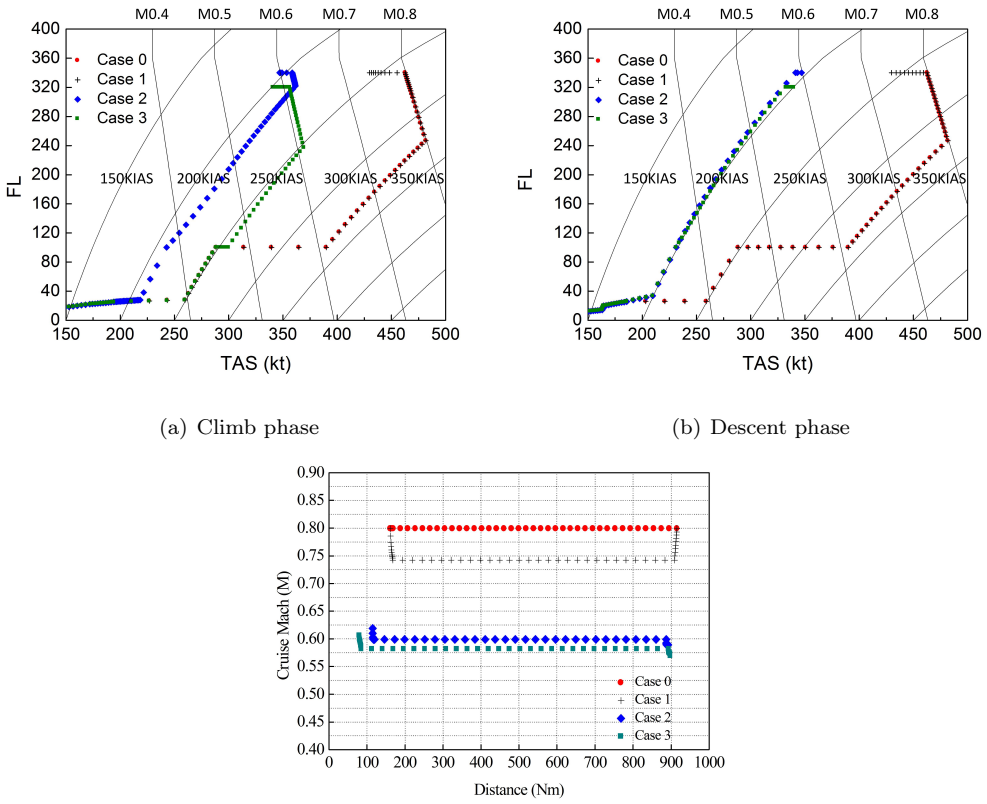

(a) Climb phase

(b) Descent phase

(c) Cruise phase

Fig. 7 Changes of speed profiles in all the Cases of study.

Fig. 7(a)), but the gained fuel (saved from climb) makes a longer delay time in cruise and descent phases since the total flight time is longer than Case-2 (see Table 1). That means, in this case, part of the delay time of climb is trade in exchange for saving more fuel.

When it comes to the cruise phase, if the fuel consumption is fixed in this phase in Case-1, then the cruise Mach decreases from M0.80 to M0.74, while the specific range keeps the same (both 0.188 nm/kg). Unlikely, in Case-2 and Case-3, the cruise Mach both reduce directly to the GD speed for each flight level, M0.60 and M0.58 respectively (see Fig. 7(c)).

As for the descent phase, we can see from Fig. 7(b) that Case-2 and Case-3 have no deceleration below FL100 (like in Case-0 and Case-1) simply because the descent speed (around 200kt) is already below the ATC constraint of IAS lower than 250kt below FL100. Meantime, the segments of constant Mach descent are both missing too, since the crossover altitudes lie higher above the cruise flight level due to the lower speed in the constant IAS descent in Case-2 and Case-3.

Normally, the fuel consumed in descent phase accounts for the lowest of the three phases, but the trade-off still generates almost double the descent time in our example (see Table 1). In Case-2, the fuel consumption grows from 107kg to 184kg, reducing the descent speed to the GD speed in descent. Remember that the GD speed is not the same in climb that in descent, since the weight of the aircraft is different (fuel has been burned in cruise).

C. Airborne delay comparison

More specific routes are further included to have a comparison on the amount of maximum airborne delay generated from different SR Cases, including FCO-CDG: 595nm, FRA-MAD: 769nm, AMS-SVQ: 1000nm and STO-ATH: 1305nm, all of which are representative of short and mid haul flights in Europe, and each is further analyzed with CI ranging from 25 to 500 kg/min. Results are summarized in Table 2.

Table 2 Analyzed flights for airborne delay comparison.

Flight Routes (Comp. time)	Case-0										Case-1		Case-2		Case-3		
	CI (kg/min)	FL (100 ft)	Time (min)	Fuel (kg)	Clb D (nm)	Clb T (min)	Crz D (nm)	Crz T (min)	Dst D (nm)	Dst T (min)	AD (min)	AD (%)	AD (min)	AD (%)	FL (100 ft)	AD (min)	AD (%)
FCO-CDG 595 Nm (10-15 Sec)	25	380	89	3464	140	21	346	47	97	17	8	16%	22	24%	380	22	24%
	60	380	86	3575	152	22	345	46	86	14	12	26%	26	30%	340	34	39%
	100	380	85	3641	160	22	338	44	85	14	10	23%	29	34%	340	37	43%
	150	380	85	3654	159	22	339	44	85	14	10	22%	30	35%	320	38	45%
	300	300	83	3991	137	19	378	48	68	12	12	24%	53	63%	260	55	66%
	500	260	83	4302	98	14	425	53	61	11	23	43%	60	73%	260	60	73%
FRA-MAD 769 Nm (10-15 Sec)	25	380	113	4334	153	23	506	68	97	17	11	16%	27	24%	380	27	24%
	60	380	110	4440	156	23	514	68	86	14	17	25%	33	30%	360	38	34%
	100	380	110	4464	152	22	519	69	86	14	14	20%	34	31%	360	39	36%
	150	340	107	4731	151	21	530	69	76	13	15	22%	52	48%	320	57	53%
	300	300	106	5030	142	19	547	70	68	12	17	25%	69	65%	280	71	68%
	500	260	104	5470	100	14	596	75	61	11	32	43%	78	75%	260	78	75%
AMS-SVQ 1000 Nm (15-20 Sec)	25	380	144	5482	161	24	729	98	97	17	16	17%	35	24%	380	35	24%
	60	380	140	5640	175	25	727	96	86	14	24	25%	44	32%	360	51	36%
	100	380	138	5768	200	27	702	92	85	14	21	23%	49	35%	340	60	43%
	150	340	137	5974	157	22	754	98	76	13	22	23%	71	52%	320	72	52%
	300	300	135	6389	147	20	772	98	68	12	25	25%	90	66%	280	90	67%
	500	260	133	6998	102	14	824	103	61	11	44	43%	104	78%	260	104	78%
STO-ATH 1305 Nm (20-30 Sec)	25	360 380	185	7054	133	20	40 991	5 133	98	17	0 23	9% 17%	42	23%	360 380	42	23%
	60	360 380	180	7242	148	21	40 988	5 131	86	14	1 37	24% 28%	62	35%	360 380	62	35%
	100	380	178	7360	210	29	997	131	85	14	31	24%	61	34%	360	71	40%
	150	340	177	7467	166	23	1050	136	76	13	51	38%	83	47%	320	86	48%
	300	300	174	7830	155	21	1069	136	68	12	59	43%	110	63%	280	110	63%
	500	260	172	9159	106	15	1126	141	61	11	59	42%	126	74%	260	126	74%

Seeing from the results of Case-0 in Table 2, with the growth of CI, the climb distance increases from CI of 25 to 100 kg/min, and then decreases gradually after greater than 150 kg/min. However,

remember in Fig. 2 that the higher the CI is, the longer the climb distance it should be. This is due to the fact the cases here in the table are resulted from a global optimization for the trajectory as a whole, while the situation in the previous figure is based on a single climb phase. The trade-off of fuel and time among different flight phases (as illustrated by the specific flight in Sec. III A) accounts for the partial inconsistent of these results.

In Case-1, it is obvious that the achievable airborne delay increases with the growth of flight route distance (i.e., the cruise distance in this case, as climb and descent phases are fixed in Case-1 in line with the nominal flight). Specifically, for each flight route, the higher CI the nominal flight chooses, the more airborne delay the flight will achieve (through the SR strategy) in general. However, we may also notice a reduction trend within the CI scope of 100 and 150 kg/min. It is because for those CIs, extra fuel is consumed in climb and descent to obtain higher speeds during the two phases, such that less fuel is left (given the total fuel kept constant) for the cruise phase, and thus a reduced amount of delay is generated.

As for Case-2, the airborne delay increases significantly only after climb and descent phases are included. If we compare the percentage that climb and descent normally account for in a flight, with the percentage that cruise has, we may find that for those short-haul flights, the distances of climb and descent may account for up to 50% while time nearly 50% too, but for the mid/long-haul flights, both distance and time percentages could reduce to about 20%. Nevertheless, most of the airborne delay in Case-2 increase to almost 3-fold of the ones in Case-1, which, as discussed in Sec. III A, is due to the fact that adding climb and descent makes it possible to re-allocate the fuel consumption in each phase, as long as the total fuel consumption remains unchanged.

When the cruise flight level is allowed to change, as Case-3, the airborne delay further increase but not so remarkable as from Case-1 to Case-2 (see Table 2). The main reason is that the specific range curves for different cruise flight levels are quite close within the low cruise speeds. As a result, the speed reduction from altitude changes, i.e., Case-2 to Case-3, will not be as large as the reduction from nominal speed to equivalent speed, i.e., Case-1 to Case-2. Typically, the new flight level would be lower than the original, but since the step interval is 2000ft, which is a discrete change due to operation constraints, some flights just keep unchanged as Case-2.

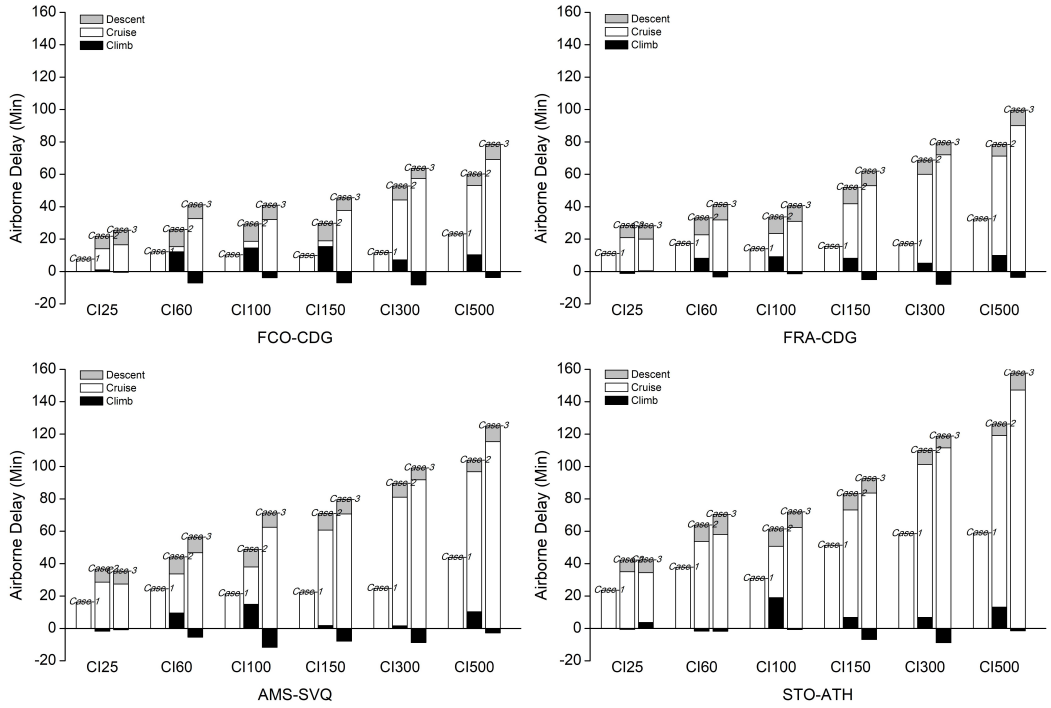

Fig. 8 Airborne delay achieved in climb, cruise and descent phases.

Fig. 8 illustrates the amount of airborne delay each phase contributes to, where in some cases negative values are observed. Worth noting these negative values are all in the climb phase of Case-3, in which the optimal cruise flight levels are lower than the nominal ones. Therefore, the altitude reduction of TOC shortens climb time, leading to a negative airborne delay.

However, this does not apply to the descent phase, given that an altitude reduction on TOD occurs as well. Since the fuel consumption in climb is typically much higher than that in descent (maximum climb thrust versus idle thrust), while the ranges of speed remains almost the same, the trade-off of fuel and time differs notably, and thus the descent phase should have a higher effect in generating airborne delay by SR with the same amount of fuel.

Finally, if the cruise flight level is not allowed to change from the nominal (Case-2), the airborne delay realized in climb can be as much as that in descent phase which keeps almost stable with regards to different CI, as shown in Fig. 8, and thus less airborne delay are generated from the cruise phase if compared with Case-3, so as to keep the total fuel consumption unchanged.

IV. Conclusions and Further Work

This paper extends previous research on linear holding strategies in cruise phases to absorb part of the ATFM delays by allowing SR on climb and descent phases too. Three different variants are analyzed, and the maximum airborne delay trajectories are computed by means of numerical optimization using an in-house trajectory generation tool, which relies on accurate performance models derived from manufacturer data.

Compared with previous works, a remarkable increase of the maximum airborne delay that can be realized without extra fuel consumption is observed. Results suggest that there exist differences on the trade-off between fuel and time in various flight phases (even in flight segments within a particular phase), and therefore including climb and descent into the SR strategy would enable the optimizer to utilize these differences to maximize the achievable time increase. Besides, the characteristics of trajectory variance resulted from performing the SR strategy has not been analyzed in this paper, and deserves a further work by including more simulation experiments.

Further work will also focus on exploring the effects of this SR strategy for the whole flight in realistic operations, as done for instance in [2]. Considering that the ATFM regulations (and the associated delays) are typically issued in response to adverse weather conditions, the wind and non-standard atmospheres, which always have great impacts on real flights, should be further taken account in regard of the application of the proposed SR strategy.

References

[1] Cook, L. S. and Wood, B., "A model for determining ground delay program parameters using a probabilistic forecast of stratus clearing," *Air traffic control quarterly*, Vol. 18, No. 1, 2010, p. 85, doi:10.2514/atcq.18.1.85.

[2] Delgado, L., Prats, X., and Sridhar, B., "Cruise speed reduction for ground delay programs: A case study for San Francisco International Airport arrivals," *Transportation Research Part C: Emerging Technologies*, Vol. 36, 2013, pp. 83–96, doi:10.1016/j.trc.2013.07.011.

[3] Ball, M. O., Hoffman, R., and Mukherjee, A., "Ground delay program planning under uncertainty based on the ration-by-distance principle," *Transportation Science*, Vol. 44, No. 1, 2010, pp. 1–14, doi:10.1287/trsc.1090.0289.

[4] Inniss, T. R. and Ball, M. O., "Estimating one-parameter airport arrival capacity distributions for air traffic flow management," *Air Traffic Control Quarterly*, Vol. 12, 2004, pp. 223–252, doi:10.2514/atcq.12.3.223.

[5] Prats, X. and Hansen, M., "Green Delay Programs: absorbing ATFM delay by flying at minimum fuel speed," in "Proceedings of the 9th USA/Europe air traffic management R&D seminar, Berlin, Germany," , 2011.

[6] Delgado, L. and Prats, X., "En route speed reduction concept for absorbing air traffic flow management delays," *Journal of Aircraft*, Vol. 49, No. 1, 2012, pp. 214–224, doi:10.2514/1.C031484.

[7] Delgado, L. and Prats, X., "Operating cost based cruise speed reduction for ground delay programs: Effect of scope length," *Transportation Research Part C: Emerging Technologies*, Vol. 48, 2014, pp. 437–452, doi:10.1016/j.trc.2014.09.015.

[8] Delgado, L. and Prats, X., "Effect of wind on operating-cost-based cruise speed reduction for delay absorption," *Intelligent Transportation Systems, IEEE Transactions on*, Vol. 14, No. 2, 2013, pp. 918–927, doi:10.1109/TITS.2013.2246864.

[9] Roberson, B. and Pilot, S. S., "Fuel Conservation Strategies: cost index explained," *Boeing Aero Quarterly*, Vol. 2, 2007, pp. 26–28.

[10] Airbus, *Getting to grips with the cost index, Issue II. Flight Operations Support and Line Assistance (STL), Customer Services Directorate, Blagnac*, 1998.

[11] Airbus, *Flight Crew Operation Manual (FCOM): A320, Version 1.3.1*, 1993.

[12] Xu, Y., Dalmau, R., and Prats, X., "Effects of speed reduction in climb, cruise and descent phases to generate linear holding at no extra fuel cost," in "Proceedings of the 7th International Conference on Research in Air Transportation (ICRAT)," , 2016.

[13] Dalmau, R. and Prats, X., "Fuel and time savings by flying continuous cruise climbs: Estimating the benefit pools for maximum range operations," *Transportation Research Part D: Transport and Environment*, Vol. 35, 2015, pp. 62–71, doi:10.1016/j.trd.2014.11.019.

[14] Betts, J. T., *Practical methods for optimal control and estimation using nonlinear programming*, Vol. 19, SIAM, 2010, doi:10.1137/1.9780898718577.